LIMNOLOGY and OCEANOGRAPHY

ASLO

Limnol. Oceanogr. 9999, 2022, 1–14

doi: 10.1002/lno.12185

The role of internal nitrogen loading in supporting non-N-fixing harmful cyanobacterial blooms in the water column of a large eutrophic lake

Daniel K. Hoffman [1*] **Mark J. McCarthy,** [2] **Ashlynn R. Boedecker,** [3] **Justin A. Myers,** [2] **Silvia E. Newell** [2]

[1]Kennesaw State University, KSU Journey Honors College, Kennesaw, Georgia
[2]Department of Earth and Environmental Sciences, Wright State University, Dayton, Ohio
[3]Department of Biology, Baylor University, Waco, Texas

Abstract

Western Lake Erie cyanobacterial harmful algal blooms (cyanoHABs) occur every summer as a result of anthropogenic nutrient loading. Although the physiological importance of nitrogen (N) in supporting bloom biomass and toxin production is established, the role of internal N recycling in the water column to support bloom maintenance is not as well understood. Over three field seasons (2015–2017), we collected water from western Lake Erie and employed bottle incubations with ^{15}N-ammonium (NH_4^+) enrichments to determine NH_4^+ regeneration and potential uptake rates in the water column. Potential NH_4^+ uptake rates followed spatial and seasonal patterns, with greatest rates measured nearest the Maumee River inflow and during peak bloom months (August and September). Regeneration followed a similar spatial pattern but was greatest in early summer (June and July) and supported ~20–60% of potential NH_4^+ demand during the height of the bloom. Basin-wide internal NH_4^+ regeneration during the April–October period could supply NH_4^+ at 60–200% of annual external N loading to the western basin. These results help explain how non-N-fixing cyanoHABs in Lake Erie and other large, eutrophic lakes continue producing biomass and N-rich toxins long after spring nutrient loads are exhausted or transported to other areas. Internal N loads are ultimately driven by external N loads; in low precipitation years, external nutrient loads result in smaller blooms, producing less substrate for subsequent internal N loads. Overall, these findings, along with others, confirm that both internal and external N loading must be considered when evaluating cyanoHAB management strategies.

Microcystis-dominated cyanobacterial harmful algal blooms (cyanoHABs) in western Lake Erie have increased in severity since the mid-1990s (Steffen et al. 2014). Research on and management of high nutrient loads from agricultural watersheds have focused on phosphorus (P) as the key driver of cyanoHABs in Lake Erie (Martin et al. 2021) and globally (Paerl et al. 2016). Although total P and total nitrogen (TN) loads have decreased in recent decades, the proportion of dissolved reactive P in the total P load to Lake Erie has increased and correlates with annual bloom size (Jarvie et al. 2017, but see River and Richardson 2019). Likewise, the fraction of the TN load comprised of chemically reduced N forms (as total Kjeldahl N [TKN]) delivered to western Lake Erie has increased concurrently and is also related to cyanoHAB biomass (Newell et al. 2019).

Uncertainties in dissolved reactive P analyses related to nanoparticulate P passing through 0.45-μm filters may result in over-estimation of Maumee River fluxes to western Lake Erie by ~ 50% (River and Richardson 2019). The temporal disconnect, exceeding the basin residence time, between spring dissolved reactive P loads and cyanoHABs in late summer is also problematic (Newell et al. 2019). In contrast, higher TKN (including highly bioavailable ammonium [NH_4^+] and urea) proportions in the Maumee River TN load in mid-summer coincide well with cyanoHAB initiation in July (Newell et al. 2019). Cyanobacteria, particularly non-N fixing taxa, are excellent at scavenging NH_4^+ and often outcompete eukaryotic organisms (e.g., diatoms) for NH_4^+ (Blomqvist et al. 1994). *Microcystis* and many other toxin-producing, bloom-forming

*Correspondence: dhoffma5@kennesaw.edu

Additional Supporting Information may be found in the online version of this article.

Author Contribution Statement: D.H. contributed to study development, collected all samples in field, conducted incubations, processed samples, analyzed data, drafted manuscript. M.M. contributed to study conception and development, sample collection, data analysis, and manuscript writing. A.B. contributed to sample and data collection, data analysis, manuscript review and editing. J.M. contributed to sample and data collection, data analysis, manuscript review and editing. S.N. contributed to study conception and development, sample collection, data analysis, and manuscript writing.

taxa (e.g., *Planktothrix*) cannot fix atmospheric dinitrogen (N_2) and thus rely on combined N, particularly NH_4^+, in the water column (Paerl et al. 2016). Maximum uptake rates (V_{max}) for NH_4^+ are 4–6 times greater than those for nitrate (NO_3^-) in *Microcystis* (Takamura et al. 1987), while diatoms are often more competitive for NO_3^- (Glibert et al. 2016).

Microcystin concentrations and biomass of non-N fixing cyanobacteria increase in response to NH_4^+ additions (Chaffin et al. 2018), and NH_4^+ and urea induce upregulation of microcystin-associated genes (Harke et al. 2016) more quickly than NO_3^- (Chaffin et al. 2018). Conversely, low NH_4^+ concentrations inhibit toxin production due to *ntcA* (global cyanobacteria N regulation gene) activation, the product of which binds to the *mcy* gene cassette responsible for microcystin production and represses its activity (Kuniyoshi et al. 2011). NH_4^+ bioreactivity leads to rapid assimilation and recycling within the sediments and water column, making it difficult to accurately characterize in situ NH_4^+ concentrations (McCarthy et al. 2013). Thus, snapshot sampling and monitoring efforts for NH_4^+ concentrations cannot accurately estimate NH_4^+ availability in situ, which requires measuring NH_4^+ assimilation and turnover/recycling rates (Gardner et al. 2017).

Over three field seasons (April through October, 2015–2017), NH_4^+ regeneration and potential uptake rates were quantified in the western Lake Erie water column to evaluate the importance of internal N loading in supporting non-N-fixing cyanoHAB biomass and toxin production. Potential NH_4^+ uptake includes both assimilation into primary producer biomass and nitrification (conversion of NH_4^+ to NO_3^-). NH_4^+ regeneration includes, but is not limited to, remineralization of organic compounds, microplankton excretions (including algal exudation), and sloppy feeding by grazers (Hopkinson et al. 1987). We also evaluated the capacity of NH_4^+ regeneration to support water column NH_4^+ demand across the bloom season relative to external TN loading.

We expected that NH_4^+ regeneration and potential uptake rates would follow patterns described previously (i.e., photic exceeding dark NH_4^+ uptake, highest NH_4^+ uptake during peak blooms, potential NH_4^+ uptake exceeding regeneration) and follow spatial and temporal trends consistent with seasonality and distance from nutrient sources. Specifically, we hypothesized that: (1) both NH_4^+ regeneration and potential uptake rates would decrease with distance from the Maumee River mouth; (2) both NH_4^+ regeneration and potential uptake rates would increase from late spring/early summer to August and September (peak bloom); and (3) rates measured in near-surface waters would be greater than those from near-bottom waters. We anticipated that the proportion of internal NH_4^+ regeneration capable of supporting potential NH_4^+ uptake would increase from bloom initiation to bloom peak. Given the importance of NH_4^+ to the metabolic demands of cyanoHABs and the difficulty of accurately determining in situ NH_4^+ concentrations, quantifying these NH_4^+ cycling pathways is critical to understanding and managing non-N-fixing cyanoHABs in western Lake Erie and other large eutrophic lakes. These kinds of measurements are exceedingly rare in the Great Lakes and other freshwater systems but are critically needed for informing and validating ecosystem models and management actions.

Materials

Field sampling

Water samples were collected in conjunction with the NOAA Great Lakes Environmental Research Laboratory (GLERL) weekly HABs monitoring program in 2015, 2016, and 2017. Further details on bloom severity, initiation, and duration are presented in supplemental material. Three stations (WE6, WE2, WE4; Fig. 1) were sampled monthly from June to September 2015 (Supporting Information Table S1), and these plus WE13 (Fig. 1) were sampled in 2016 and 2017 during May–October (with an additional sampling at WE2 in April 2016). These stations represent a spatial and depth gradient moving away from the Maumee River inflow. Not all stations were sampled during each month, and sampling varied across years due to opportunity and weather constraints, particularly in 2016, when frequent storms interrupted scheduled sampling events. At each station, water was collected from two depths ($\sim$ 1 m below the surface and $\sim$ 1 m above the sediment–water interface) with a 5-L Niskin bottle. Ten L of water were collected from each depth and transferred into 20-L polyethylene carboys. Twelve ml of ambient nutrient (orthophosphate [o-PO_4^{3-}], NH_4^+, urea, nitrite [NO_2^-], NO_3^-) samples were filtered immediately on-site (0.22-μm Nylon filters) into 15-ml polypropylene sample tubes and frozen in the field (dry ice) until transfer into a -20°C lab freezer. Other biological and physicochemical parameters (water temperature, dissolved oxygen, total P, Secchi depth, conductivity, photosynthetically active radiation (PAR), turbidity, total suspended solids (TSS), and chlorophyll *a* (Chl *a*), phycocyanin, and microcystin concentrations) were collected from surface waters and analyzed by NOAA GLERL and CIGLR (NOAA Great Lakes Environmental Research Laboratory; Cooperative Institute for Great Lakes Research, University of Michigan, 2019). All physicochemical data other than nutrients are available in supplemental material. The N and P mass of Maumee River loads was obtained from the National Center for Water Quality Research (NCWQR) database, and other ambient environmental characteristics of interest (average daily wind speed, wind direction, air temperature) were selected from buoy data hosted by NOAA's National Data Buoy Center (https://www.ndbc.noaa.gov; last accessed 30 November 2020) and Michigan Technological University's Upper Great Lakes Observing System (http://uglos.mtu.edu; last accessed 30 November 2020).

Incubations

NH_4^+ regeneration and potential uptake rates were quantified via enrichment with ^{15}N-labeled NH_4^+ (McCarthy

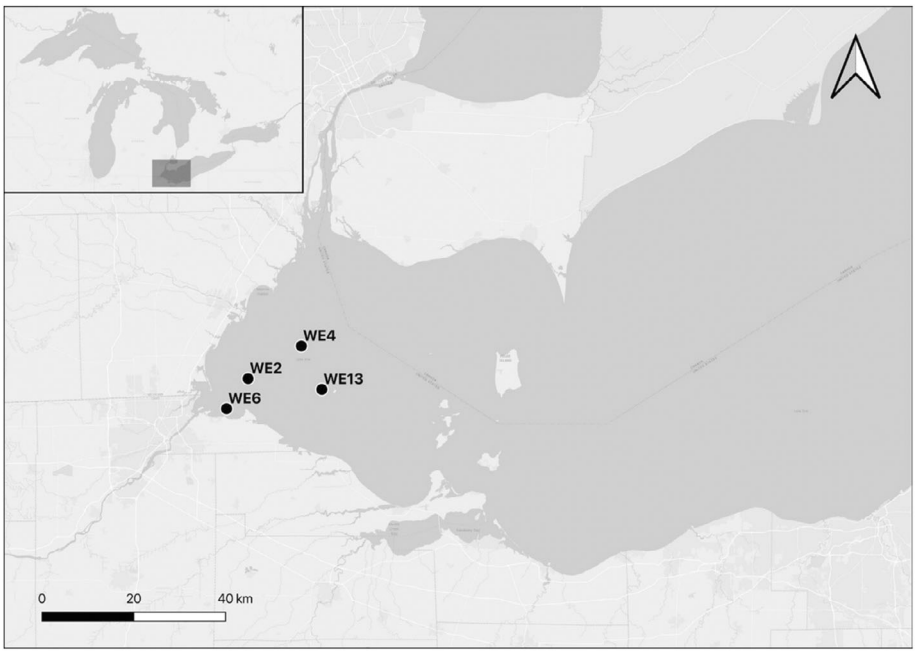

Fig. 1. Western Lake Erie sampling stations. Stations are located at the following coordinates (latitude, longitude): WE6 (41.70555, −83.386533), WE2 (41.7638, −83.330617), WE4 (41.8269833, −83.192117), and WE13 (41.7429167, −83.138783).

et al. 2013). One-L aliquots of water from each station and depth were amended with $^{15}NH_4Cl$ (98 atom % ^{15}N, Sigma Aldrich; final concentration 8–24 μM, depending on sampling date and bloom conditions; Supporting Information Table S1), mixed, and distributed among six clear, colorless, 125-mL Nalgene bottles for triplicate light and dark (foil-wrapped) incubations. Initial samples from each bottle were collected immediately using a syringe and canula, filtered (0.22 μm), and frozen at −20°C until analysis. Bottles were incubated in a mesh bag for 16–25 h (Supporting Information Table S1) in simulated ambient lake conditions (outdoor water bath, not temperature-controlled) before being filtered (0.22 μm) into 15-mL polypropylene sample tubes and immediately frozen at −20°C until total NH_4^+ analysis ($^{14}N + {}^{15}N$). Pre- and post-incubation samples for $^{15}NH_4^+$ analyses were filtered into 12-mL Exetainers (Labco) with no headspace, sealed with double-wadded septa caps, and stored in the dark at room temperature (17°C) until analysis (within 1 week).

Sample analysis and rate calculations

Total NH_4^+ concentrations were determined via colorimetric flow-injection analysis (Lachat Quikchem 8500). $^{15}NH_4^+$ concentrations were quantified via OX-MIMS (Yin et al. 2014). Additional details on OX-MIMS are provided in supplemental material. Total NH_4^+ concentrations were used to determine the $^{15}NH_4^+$ to total NH_4^+ ratio for use in isotope dilution models (Blackburn 1979; Caperon et al. 1979). Potential NH_4^+ uptake rates were qualified as potential rates due to saturating-level isotope additions (McCarthy et al. 2013), but rates determined from saturating-level isotope amendments tend to converge with actual rates in highly productive aquatic systems (Glibert et al. 1988).

In August 2015, $^{15}NH_4^+$ was undetectable after 21 h of incubation. However, a clear decrease (up to 50%) in $^{15}NH_4^+$ concentration was observed between the known amendment and initial sampling (~15 min). Therefore, we calculated NH_4^+ regeneration and potential uptake rates for the abbreviated period. Rates for one station near WE6 were measured from a separate sampling event 5 d prior to the others, and these data are included in supplemental materials and briefly mentioned in the Discussion section, but not included in any statistical analyses.

Statistical analyses

All analyses were performed in R (version 3.6.1; R Core Team 2020). Rate data were visually examined for assumptions of normality and heteroscedasticity and via Shapiro–Wilk tests; all failed to meet normality assumptions, so they were log-transformed prior to analysis. All linear models were conducted with the *lm* function from the "lme4" package (Bates et al. 2015). Differences among treatment means were determined via Tukey's HSD post hoc tests using the *emmeans* function from the "emmeans" package (Lenth et al. 2019). More detail about linear models can be found in supplemental material.

Spearman's Rank correlations were calculated using the *rcorr* function from "Hmisc" package (Harrell 2019) to inform relationships between NH_4^+ regeneration and potential

uptake and environmental variables. For correlations, we added bloom day, defined as days plus or minus the bloom initiation day (as determined by the first report of cyanobacteria in NOAA GLERL HABs bulletins), as a variable.

Results

Ambient conditions

NH_4^+ concentrations peaked in June and decreased through the bloom season (Table 1), also decreasing along the distance gradient from the river input. $NO_3^- + NO_2^-$ (NO_x) concentrations were usually 5–65 times greater than NH_4^+ and followed a similar spatial trend, with peak NO_x concentrations observed near the Maumee River discharge. NO_x concentrations generally peaked later than NH_4^+ concentrations before decreasing to less than 1 μM at the westernmost stations late in the sampling season. Urea concentrations followed similar patterns to those for NH_4^+, with higher concentrations in June decreasing through the sampling season. o-PO_4^{3-} concentrations in the westernmost part of the basin decreased from mid-summer until bloom initiation. High o-PO_4^{3-} concentrations (5–20 μM) were observed in surface waters in September 2015, despite most N forms being depleted. o-PO_4^{3-} concentrations in 2016 did not exhibit the decreasing trend observed in the other two years.

Phycocyanin (cyanobacteria) and Chl *a* (Table 2) followed similar patterns during each year and sampling season, peaking at WE6 in August, when ambient NH_4^+ concentrations were at or near undetectable levels. Maximum Chl *a* and phycocyanin in 2017 were 1.5–2 times those from the same stations in 2015, although these peak values represent samples from just below the surface, not within surface scums. Chl *a* was correlated with bloom day, all N forms (except NO_2^- and TN), the TN mass and N:P ratio of the previous week's Maumee River load, Secchi depth, water temperature, PAR, turbidity, TSS, and both dissolved and particulate microcystins (Supporting Information Table S2). Phycocyanin was similarly correlated with bloom day, all N forms (except TN), the TN mass and N : P ratio of the Maumee River load from the previous week, Secchi depth, turbidity, TSS, and both toxin measures, but was additionally correlated with wind speed (Supporting Information Table S2). Particulate and dissolved microcystin concentrations followed similar spatial and temporal trends in 2016 and 2017, with maximum values at WE6 in August. In 2015, maximum dissolved and particulate microcystins were observed at WE6 in September and WE2 in August. In 2017, peak particulate microcystins (21.6 $\mu g\,L^{-1}$) were measured at WE6 in August, coinciding with Chl *a* and phycocyanin maxima. Both dissolved and particulate microcystins were correlated with bloom day, several N concentrations (NH_4^+, NO_3^-, total dissolved N, dissolved inorganic N (DIN), and particulate organic N), the TN mass of the Maumee River load from the previous week, TSS, Chl *a*, and phycocyanin (Supporting Information Table S2). Neither biomass nor toxin concentrations were correlated with any P form.

Potential NH_4^+ uptake

Potential NH_4^+ uptake rates were not influenced by depth across station ($F_{9,231} = 1.38$; $p = 0.196$), month ($F_{7,233} = 6.07$; $p = 0.129$), or year ($F_{3,237} = 11.8$; $p = 0.572$), so surface and bottom rates were averaged. Light NH_4^+ uptake rates closest to the Maumee River mouth (WE6 and WE2) were greater than at WE4 or WE13 ($F_{3,327} = 29.2$; $p < 0.001$), but rates at WE6 and WE2, and WE4 and WE13, were not different from each other (Fig. 2a). Light NH_4^+ uptake rates were different across months ($F_{6,324} = 12.8$; $p < 0.001$), with highest rates in August 2015 (Fig. 2b). Disregarding August 2015, the effect of month was still robust, but August was no longer different from June, July, or September ($F_{6,306} = 5.24$; $p < 0.001$; Fig. 3a). Neither spatial (station) nor yearly patterns changed from adjusting linear model input. Across all months (excluding August 2015), light NH_4^+ uptake was different year-to-year ($F_{2,328} = 58.8$; $p < 0.001$). Uptake rates were greater in 2015 than 2016 or 2017, but light NH_4^+ uptake rates in 2016 and 2017 were not different from each other (Fig. 3b).

Dark NH_4^+ uptake rates were not different between WE2 and WE6 or WE4, but rates at all of these stations were higher than WE13 ($F_{3,327} = 13.1$; $p < 0.001$; Fig. 2a). Dark NH_4^+ uptake did not differ between months ($F_{6,306} = 1.14$; $p = 0.338$; Fig. 3a) and were also greater in 2015 than 2016 or 2017 ($F_{2,328} = 32.2$; $p < 0.001$; Fig. 3b).

Excluding August, light and dark NH_4^+ uptake rates in 2015 ranged from undetectable to 1.48 $\mu mol\,N\,L^{-1}\,h^{-1}$ and undetectable to 0.772 $\mu mol\,N\,L^{-1}\,h^{-1}$ (Fig. 3b; Supporting Information Fig. S1), respectively. The greatest rates (light = 20.2 $\mu mol\,N\,L^{-1}\,h^{-1}$, dark = 24.4 $\mu mol\,N\,L^{-1}\,h^{-1}$) were observed in August at WE6 and WE2. NH_4^+ uptake rates were generally higher at these stations than at WE4 (Supporting Information Fig. S1). In 2016, light and dark NH_4^+ uptake rates ranged from undetectable to 0.775 $\mu mol\,N\,L^{-1}\,h^{-1}$ and undetectable to 0.334 $\mu mol\,N\,L^{-1}\,h^{-1}$, respectively (Fig. 3b; Supporting Information Fig. S2). Rates in 2016 peaked at WE6 in July and August and WE2 in August. By October, rates had nearly returned to those observed in May and June (Supporting Information Fig. S2). In 2017, light and dark NH_4^+ uptake ranged from 0.011 to 1.10 $\mu mol\,N\,L^{-1}\,h^{-1}$ and undetectable to 0.934 $\mu mol\,N\,L^{-1}\,h^{-1}$, respectively (Fig. 3b; Supporting Information Fig. S3). Rates at WE6 peaked in August, which were the highest 2017 rates except WE2 in June (Supporting Information Fig. S3).

Across the entire dataset, light and dark NH_4^+ uptake rates were correlated with many physicochemical parameters, including several nutrient forms (TN, particulate organic N), both biomass parameters, and microcystin concentrations (Supporting Information Table S2).

Table 1. Nutrient concentrations (μmol N or P L^{-1}) for ammonium (NH_4^+), nitrite (NO_2^-), nitrate (NO_3^-), orthophosphate (o-PO_4^{3-}), and urea near the water surface.

Date	Station	NH_4^+ (μM)	NO_2^- (μM)	NO_3^- (μM)	o-PO_4^{3-} (μM)	Urea (μM)
22 Jun 2015	WE6	7.01	1.21	260	4.10	2.71
	WE2	4.03	0.320	315	1.31	1.35
	WE4	0.646	0.120	22.0	0.040	1.18
20 Jul 2015	WE6	5.36	1.93	196	4.19	2.71
	WE2	1.45	2.17	216	3.27	1.44
	WE4	BDL	1.58	49.5	0.040	0.692
10 Aug 2015	WE6	BDL	0.740	91.2	0.510	0.470
	WE2	BDL	0.730	99.0	1.21	0.310
	WE4	BDL	0.260	4.98	0.050	0.310
28 Sep 2015	WE6	0.650	BDL	0.032	5.56	0.500
	WE2	4.86	BDL	0.024	20.7	0.500
	WE4	0.300	BDL	0.014	6.92	1.50
19 Apr 2016	WE2	4.21	0.730	45.6	0.170	0.450
30 May 2016	WE4	1.72	BDL	9.50	0.050	0.600
	WE13	6.04	0.370	15.1	0.600	0.400
27 Jun 2016	WE6	9.72	1.57	48.8	1.35	2.08
	WE2	5.49	0.500	26.1	0.280	0.560
	WE4	0.54	0.410	11.9	0.010	0.410
11 Jul 2016	WE6	0.250	7.40	326	0.080	0.650
	WE2	2.10	0.870	30.6	0.130	0.390
	WE4	0.670	0.560	18.0	0.060	0.250
08 Aug 2016	WE6	0.020	0.130	4.97	0.060	0.490
	WE2	0.420	0.570	12.1	0.040	0.300
	WE4	BDL	0.790	8.84	0.050	0.570
	WE13	0.840	0.200	5.40	0.070	1.30
19 Sep 2016	WE6	0.800	0.510	9.49	0.790	2.10
	WE2	2.41	0.710	5.78	0.890	0.770
17 Oct 2016	WE4	1.86	0.430	19.0	0.570	0.470
	WE13	0.950	2.56	7.82	1.13	0.560
	WE6	1.87	0.650	29.5	0.800	1.20
	WE2	0.430	0.740	20.0	0.380	0.360
30 May 2017	WE6	6.48	4.88	373	4.51	2.86
	WE2	2.87	4.85	314	2.65	2.26
	WE4	4.63	0.290	34.2	0.030	0.355
	WE13	1.88	0.450	36.8	0.040	0.423
12 Jun 2017	WE6	7.30	4.94	352	4.10	2.71
	WE2	1.55	3.63	230	1.31	1.35
	WE4	2.75	0.540	40.0	0.040	1.18
	WE13	2.11	0.270	33.4	0.040	0.553
17 Jul 2017	WE6	6.29	5.13	400	4.32	2.71
	WE2	2.55	5.38	364	2.89	1.44
	WE4	2.52	1.10	42.6	0.080	0.692
	WE13	0.760	0.860	37.5	0.090	0.501
14 Aug 2017	WE6	0.330	1.46	122	0.530	0.820
	WE2	0.290	0.450	34.8	0.060	0.722
	WE4	0.720	1.65	77.0	0.090	0.446
	WE13	0.800	1.00	51.4	0.030	0.368

(Continues)

Table 1. Continued

Date	Station	NH_4^+ (μM)	NO_2^- (μM)	NO_3^- (μM)	o-PO_4^{3-} (μM)	Urea (μM)
18 Sep 2017	WE6	0.270	BDL	0.390	0.040	0.536
	WE2	BDL	0.020	0.700	0.063	0.290
	WE4	0.290	1.19	18.9	0.038	0.345
	WE13	0.260	0.030	0.990	0.039	0.424
10 Oct 2017	WE6	BDL	0.020	0.390	0.170	0.539
	WE2	0.040	0.050	0.450	0.210	0.340
	WE4	0.630	0.720	20.7	0.180	0.326
	WE13	0.150	0.480	15.7	0.060	0.219

BDL, below method detection limit.

For the entire dataset, light exceeded dark NH_4^+ uptake at all stations ($F_{7,654} = 21.4$; $p < 0.001$), in June–October ($F_{13,648} = 9.61$; $p < 0.001$), and within each year (includes April and May; $F_{5,656} = 40.6$; $p < 0.001$). There were instances (usually WE4 and WE13) where dark NH_4^+ uptake rates were comparable to or exceeded light rates, particularly in July (Supporting Information Figs. S1–S3).

NH_4^+ regeneration

Light and dark NH_4^+ regeneration rates were not different ($F_{1,660} = 0.637$; $p = 0.425$), so they were averaged together for each incubation. Across all sampling dates, NH_4^+ regeneration exhibited differences by station ($F_{3,327} = 11.8$; $p < 0.001$) and was greatest at WE6 and WE2, but rates at WE6 and WE2 were not different from each other (Fig. 4a). NH_4^+ regeneration rates were also different when evaluated by month ($F_{6,306} = 5.86$; $p < 0.001$), with highest regeneration rates in June and July (Fig. 5a). NH_4^+ regeneration rates also varied across years ($F_{2,328} = 38.5$; $p < 0.001$), with 2015 rates (even excluding August 2015) greater than 2016 or 2017, while the latter two years were not different from each other (Fig. 5b).

NH_4^+ regeneration rates peaked in August 2015 (13.0 μmol N L^{-1} h^{-1}; Fig. 4b), ranging from undetectable to 0.650 μmol N L^{-1} h^{-1} across the rest of 2015 (Fig. 5b; Supporting Information Fig. S4). NH_4^+ regeneration rates in 2016 ranged from undetectable to 0.282 μmol N L^{-1} h^{-1}, peaking at WE6 in July and WE2 in August, before declining in September (Fig. 5b; Supporting Information Fig. S5). In 2017, rates ranged from undetectable to 0.289 μmol N L^{-1} h^{-1} and remained low until mid-summer, reaching a maximum at WE6 in August (Fig. 5b; Supporting Information Fig. S6).

NH_4^+ regeneration rates were negatively correlated with Secchi depth and positively related to light and dark NH_4^+ uptake, water and air temperature, conductivity, turbidity, TSS, phycocyanin, Chl *a*, particulate microcystins, total P, particulate organic N, and TN (Supporting Information Table S2).

The capacity of water column NH_4^+ regeneration to support community NH_4^+ demand in western Lake Erie exhibited similar patterns in each year, peaking in June (82.4–124%) and decreasing through August (Supporting Information Fig. S7a), when TN loads from the Maumee River watershed decreased (Supporting Information Fig. S7b). Water column nutrient concentrations (Table 1) and external TN loads (Supporting Information Fig. S7b) were low during peak bloom months (August and September), while NH_4^+ regeneration continued at rates supporting ~20–60% of community NH_4^+ demand, providing an internal N load not accounted for in external loading or water column concentration measurements.

Discussion

This study (2015–2017) quantified NH_4^+ cycling rates in western Lake Erie along a spatial gradient from the primary nutrient source (Maumee River) into the main basin and assessed the role of internal NH_4^+ dynamics in supporting cyanoHABs. Our results help explain the persistence of high biomass and toxin concentrations despite N depletion.

Water column NH_4^+ cycling

We did not observe depth-driven differences for any rate measurement. Western Lake Erie is shallow and well mixed, and *Microcystis* can regulate buoyancy and migrate vertically in the water column (Wallace et al. 2000), perhaps explaining this observation. While extreme for Lake Erie, NH_4^+ regeneration and potential uptake rates measured in August 2015 were similar to maxima reported during a cyanoHAB in Lake Smith, Alaska (15.4 μmol L^{-1} h^{-1}; Gu and Alexander 1993). At WE6 in August 2015, extracted phycocyanin and Chl *a* values from surface scums were 1700 and 1900 μg L^{-1}, respectively (NOAA Great Lakes Environmental Research Laboratory; Cooperative Institute for Great Lakes Research, University of Michigan, 2019), and NH_4^+ concentrations were near-undetectable (Table 1). NH_4^+ regeneration and potential uptake rates measured at a station < 1 km from WE6 five days prior (Supporting Information Fig. S8) were nearly two orders of magnitude less than our highest values, but approximately half of potential NH_4^+ uptake rates at WE6 in August 2016 and 2017, reflecting spatial and temporal variability in bloom biomass (Chaffin et al. 2021).

Table 2. Ambient biological and cyanotoxin (microcystins) concentrations in surface waters.

Date	Station	Phycocyanin (μg/L)	Chl *a* (μg L^{-1})	Dissolved microcystins (μg L^{-1})	Particulate microcystins (μg L^{-1})
22 Jun 2015	WE6	0.155	1.63	BDL	BDL
	WE2	0.218	3.84	BDL	BDL
	WE4	0.389	1.01	BDL	BDL
20 Jul 2015	WE6	0.450	2.88	BDL	BDL
	WE2	BDL	6.59	BDL	BDL
	WE4	155	120	0.150	8.46
10 Aug 2015	WE6	241	353	0.150	3.10
	WE2	46.8	187	0.150	9.19
	WE4	9.89	86.3	0.280	2.29
28 Sep 2015	WE6	51.8	55.0	0.340	1.99
	WE2	22.4	28.0	0.140	0.910
	WE4	17.6	22.2	0.210	0.260
19 Apr 2016	WE2	—	—	—	—
30 May 2016	WE4	0.36	2.60	BDL	BDL
	WE13	0.24	4.80	BDL	BDL
27 Jun 2016	WE6	0.993	4.25	BDL	BDL
	WE2	0.122	4.03	BDL	BDL
	WE4	0.105	4.31	BDL	BDL
11 Jul 2016	WE6	4.46	36.0	0.155	0.547
	WE2	0.453	4.14	BDL	0.137
	WE4	0.131	1.82	BDL	BDL
08 Aug 2016	WE6	14.6	62.2	0.300	4.70
	WE2	4.20	39.1	0.210	3.02
	WE4	0.251	7.77	0.110	0.270
	WE13	7.79	7.20	0.140	2.27
19 Sep 2016	WE6	6.02	8.80	0.280	1.41
	WE2	0.312	5.52	0.130	0.210
17 Oct 2016	WE4	0.056	2.71	0.100	0.010
	WE13	0.300	8.09	0.220	0.140
	WE6	0.164	0.400	0.190	BDL
	WE2	0.239	5.20	0.150	BDL
30 May 2017	WE6	0.098	2.98	BDL	BDL
	WE2	0.092	2.56	BDL	BDL
	WE4	BDL	2.45	BDL	BDL
	WE13	0.167	10.1	BDL	BDL
12 Jun 2017	WE6	BDL	3.41	0.110	BDL
	WE2	0.079	26.9	0.099	BDL
	WE4	BDL	7.61	0.109	BDL
	WE13	BDL	1.94	0.250	BDL
17 Jul 2017	WE6	0.103	3.25	BDL	BDL
	WE2	0.461	19.8	BDL	BDL
	WE4	BDL	2.18	0.100	BDL
	WE13	BDL	3.16	BDL	BDL
14 Aug 2017	WE6	453	532	0.590	21.6
	WE2	23.2	27.1	0.140	4.00
	WE4	19.3	30.6	0.370	3.70
	WE13	2.37	12.4	0.130	0.320

(Continues)

Table 2. Continued

Date	Station	Phycocyanin (μg/L)	Chl *a* (μg L^{-1})	Dissolved microcystins (μg L^{-1})	Particulate microcystins (μg L^{-1})
18 Sep 2017	WE6	19.3	33.5	0.180	0.760
	WE2	68.7	35.1	0.180	0.300
	WE4	4.75	9.62	0.230	0.250
	WE13	109	53.1	BDL	0.550
10 Oct 2017	WE6	26.1	40.9	0.210	0.560
	WE2	16.8	27.7	BDL	0.450
	WE4	0.423	5.11	BDL	BDL
	WE13	9.86	14.5	BDL	0.160

BDL, below method detection limit.

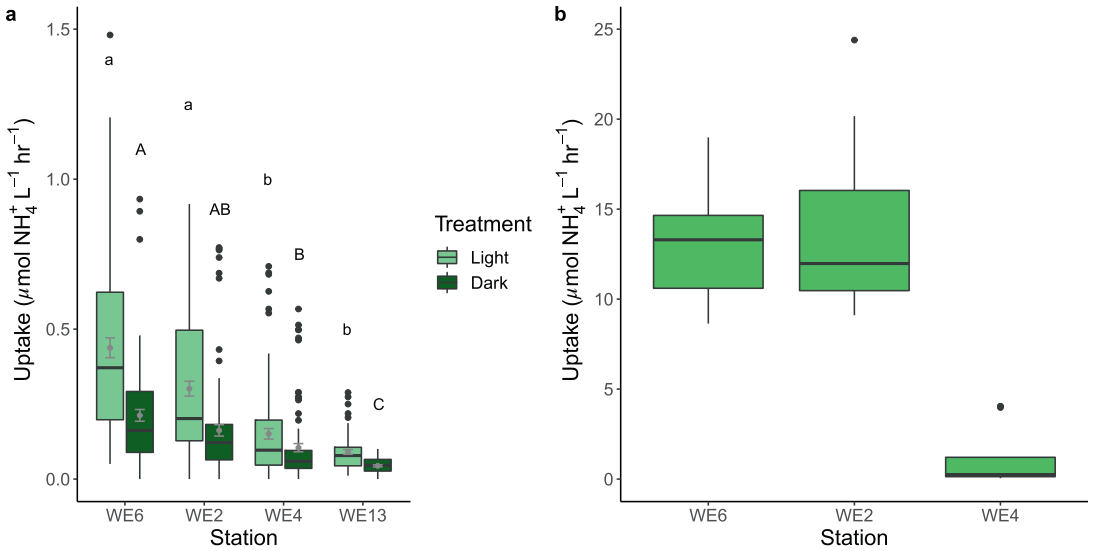

Fig. 2. Potential NH_4^+ uptake rates (μmol L^{-1} h^{-1}) (**a**) in light and dark incubations across all sampling events by station, and (**b**) August 10, 2015 (no light/dark due to abbreviated incubation; note difference in *y*-axis scale). Means (± SE) are overlaid on each boxplot in **(a)** in gray. Letters reflect differences in uptake rates between stations (Tukey's HSD post hoc tests) within each treatment (lowercase letters for light, uppercase letters for dark). *n* for each station: WE6 = 90, WE2 = 95, WE4 = 87, WE13 = 60.

Potential NH_4^+ uptake rates were greater in the light than dark, indicating expected photoautotrophic activity when light and NH_4^+ were available. Potential NH_4^+ uptake rates across both light and dark treatments were similar to but sometimes exceeded rates reported in other eutrophic systems, including Lake Champlain (Missisquoi Bay; McCarthy et al. 2013) and Lake Okeechobee (James et al. 2011). These rates were often much greater than those reported in Lake Balaton (Présing et al. 2001), Lake Michigan (Gardner et al. 2004), Lake Superior (Kumar et al. 2008), and several orders of magnitude greater than those previously reported in Lake Erie (Murphy 1980). In addition to differences in methodology, this large discrepancy is almost certainly explained by greatly reduced phytoplankton biomass following aggressive nutrient load mitigation strategies in the years prior to the study (Watson et al. 2016). Greater light NH_4^+ uptake rate maxima were reported in hypereutrophic Lake Taihu (Hampel et al. 2018), as well as in *Planktothrix*-dominated Sandusky Bay in Lake Erie (Hampel et al. 2019*a*), Lake Okeechobee (Hampel et al. 2019*b*), and subarctic Smith Lake in Alaska (Gu and Alexander 1993).

Maximal NH_4^+ regeneration rates in western Lake Erie were similar to those reported for Lake Okeechobee (James et al. 2011) and Missisquoi Bay (Lake Champlain; McCarthy et al. 2013), as well as an Amazon floodplain lake (Morrissey and Fisher 1988). NH_4^+ regeneration rate maxima in western

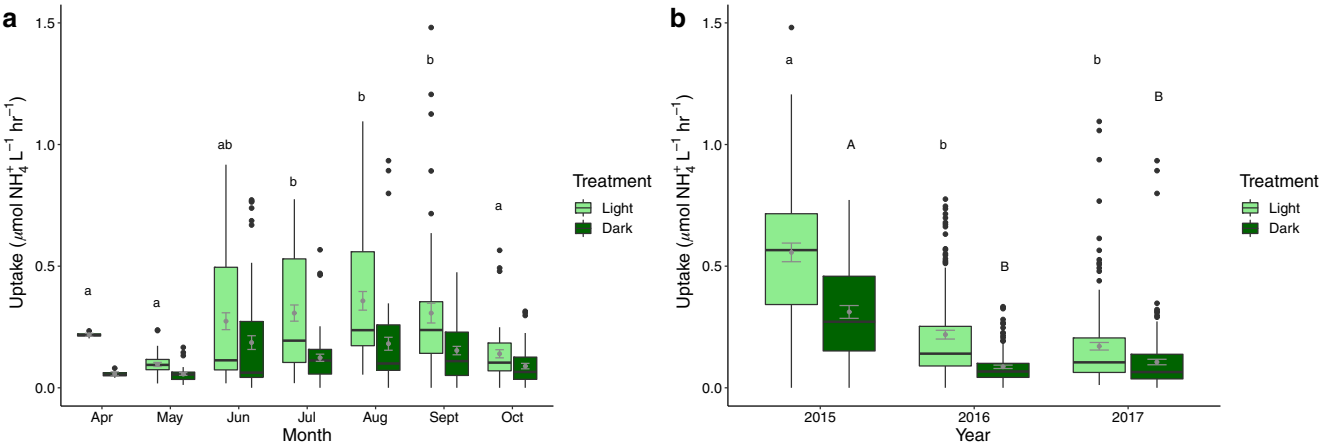

Fig. 3. (**a**) Potential NH_4^+ uptake rates (μmol L^{-1} h^{-1}) in the light (light green) and dark (dark green) for each month across all 3 yr (August 2015 excluded). Means (± SE) are overlaid on each boxplot in gray. Letters indicate differences in uptake rates between months (Tukey's HSD post-hoc tests) in the light treatment; there were no differences in dark rates across months. *n* for each month: April = 6 May = 36 June = 66 July = 57 August = 66-September = 53 October = 48. (**b**) Potential NH_4^+ uptake rates (μmol L^{-1} h^{-1}) in the light (light green) and dark (dark green) across all 3 yr (August 2015 excluded). Means (± SE) are indicated on each boxplot in gray. Letters indicate differences in uptake rates between years (Tukey's HSD post hoc tests); yearly differences in each treatment (light and dark) were the same. *n* for each year: 2015 = 71, 2016 = 117, 2017 = 144).

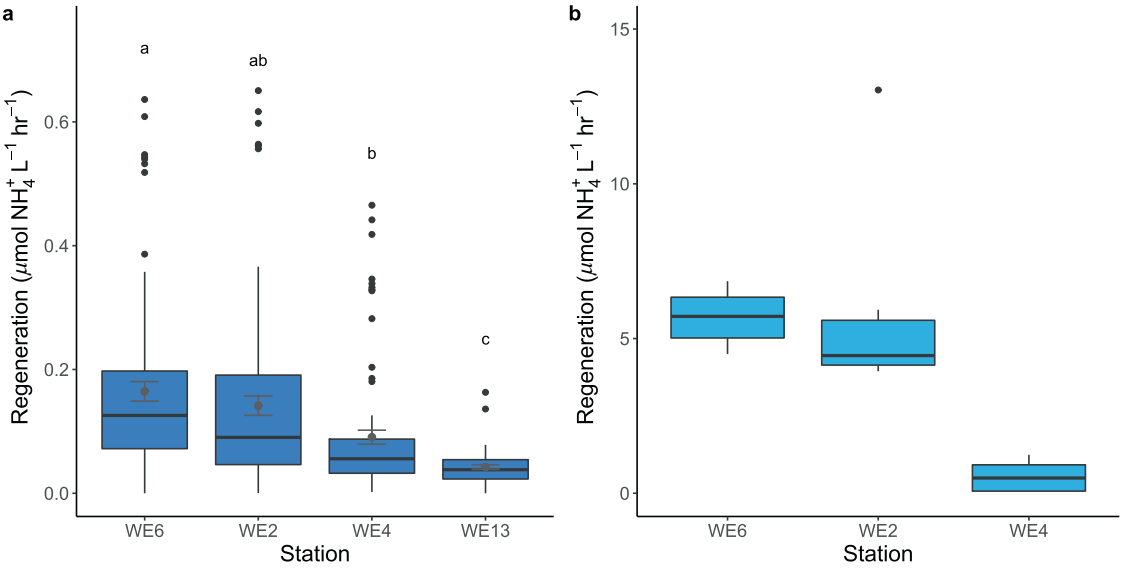

Fig. 4. NH_4^+ regeneration rates (μmol L^{-1} h^{-1}) (**a**) across all months and years by sampling station; and (**b**) from August 14, 2015 (note difference in *y*-axis scale). Means (± SE) are overlaid on each boxplot in **(a)** in gray. Letters indicate differences in regeneration rates between sites (Tukey's HSD post hoc tests). *n* for each station: WE6 = 90, WE2 = 95, WE4 = 87, WE13 = 60.

Lake Erie were two orders of magnitude greater than those from Lake Michigan (Gardner et al. 2004), up to an order of magnitude less than those in Sandusky Bay (Hampel et al. 2019*a*) and Lake Okeechobee (Hampel et al. 2019*b*), and 3–5 times less than those from Lake Taihu (McCarthy et al. 2007; Jiang et al. 2019) and Petit Saut Lake (French Guyana; Collos et al. 2001). In general, NH_4^+ regeneration and potential uptake rates in this study fell within the range of those reported for other eutrophic lakes and measured using similar methods.

The hypothesis that community NH_4^+ uptake and turnover rates would decrease with distance from the Maumee River inflow was supported by the results. WE4 and WE13 had lower rates than the westernmost stations, indicating less demand and recycling further from the nutrient source. We also predicted greater NH_4^+ uptake rates during peak bloom months, and although there was no difference between summer months (June–September) once August 2015 values were disregarded, positive relationships between light NH_4^+ uptake, temperature, phycocyanin, and Chl *a* support this prediction.

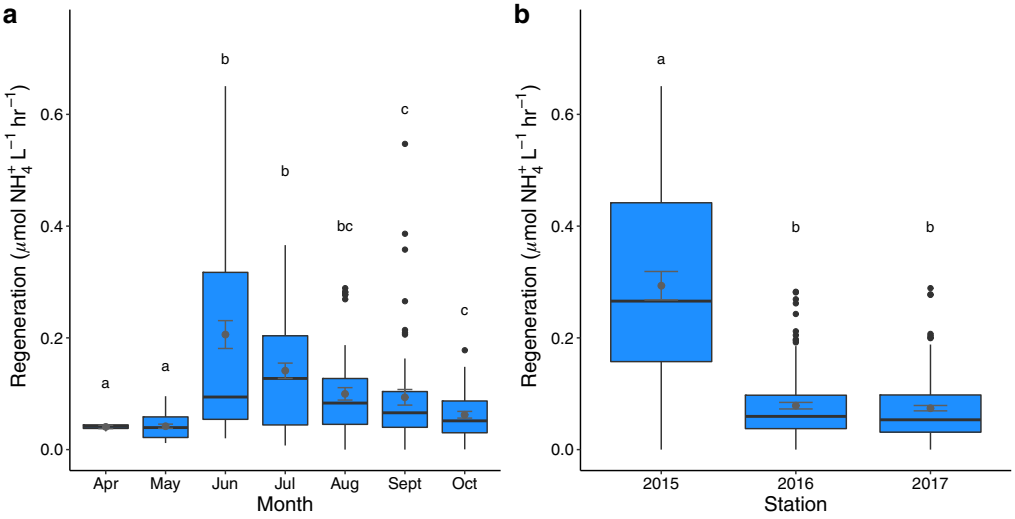

Fig. 5. (a) NH_4^+ regeneration rates (μmol L^{-1} h^{-1}) by month across all sampling years (excluding August 2015). *n* for each month: April = 6 May = 36-June = 66 July = 57 August = 66 September = 53 October = 48. (b) NH_4^+ regeneration rates (μmol L^{-1} h^{-1}) by year (excluding August 2015). *n* for each year: 2015 = 71, 2016 = 117, 2017 = 144. Means (± SE) are overlaid on each boxplot in gray. Letters indicate differences in regeneration rates between (**a**) months or (**b**) years (Tukey's HSD post hoc tests).

Contrary to our prediction, NH_4^+ regeneration could not fully support potential NH_4^+ demand during peak bloom periods (Supporting Information Fig. S7). This result agrees with findings from Lake Champlain (McCarthy et al. 2013) but contrasts with *Microcystis*-dominated Lake Taihu, where summer NH_4^+ regeneration rates could support 100% of community NH_4^+ demand (Hampel et al. 2018). Unlike Lake Erie, NH_4^+ is detectable in Taihu in August, and the external N load is much greater (Hampel et al. 2018). High NH_4^+ regeneration rates we report here represent a large, continuous NH_4^+ supply to support cyanoHAB biomass and toxin production, especially during peak biomass months (August and September), when cyanoHABs in Lake Erie are N-stressed (Chaffin et al. 2018). N stress also decreases intracellular concentrations of N-rich microcystins (Van de Waal et al. 2014). Our data suggest that toxin production during this period required regenerated NH_4^+. Sediment–water interface N effluxes also supply bioavailable N to supplement water column NH_4^+ regeneration and external loading (Présing et al. 2008; McCarthy et al. 2016), as shown recently for the same study area of Lake Erie (Boedecker et al. 2020).

Throughout the study, the 2015 bloom was the most severe in terms of biomass and areal coverage, followed by 2017 and 2016 (NOAA; Wynne et al. 2021; further description in Supporting Information). Even excluding August 2015 rates, 2015 exhibited higher potential NH_4^+ uptake rates than other years. N concentrations and cyanobacteria biomass were inversely related (Supporting Information Table S2), but neither biomass proxy was related to o-PO_4^{3-} concentration. This pattern reflects seasonal cyanoHAB maxima, where bioavailable N became depleted by non-N-fixing *Microcystis* (Table 1). High TKN : TN ratios in the Maumee River load coincide with bloom formation in mid-July, several months after spring P loads (Newell et al. 2019). *Microcystis*-dominated blooms in

Table 3. Extrapolated NH_4^+ regeneration in the water column vs. annual (a) or sampling season (b) TN load (in metric tons): 2015 sampling season June–September, 2016 April–October, and 2017 May–October. Regenerated NH_4^+ values in 2015 include those generated from very high rates in August.

(a)	Regenerated NH_4^+	TN annual load	% of annual load
2015	8.15×10^4	3.79×10^4	215
2016	1.64×10^4	2.72×10^4	60.3
2017	2.40×10^4	3.87×10^4	62.0
(b)	Regenerated NH_4^+	TN sampling season load	% of seasonal load
2015	8.15×10^4	1.80×10^4	452
2016	1.64×10^4	1.05×10^4	156
2017	2.40×10^4	1.85×10^4	130

the western basin originated in the mid-1990s (Steffen et al. 2014), coinciding with the increased proportion of TKN (Newell et al. 2019), while increased dissolved reactive P loads did not occur until after 2002 (Jarvie et al. 2017). Combined with reported over-estimation of Maumee River dissolved reactive P loads (River and Richardson 2019), the focus on dissolved reactive P loads as the main driver of cyanoHABs in Lake Erie (e.g., Annex 4 of the Great Lakes Water Quality Agreement, IJC) is insufficient.

Scaling up: NH_4^+ regeneration in western Lake Erie

CyanoHAB biomass and toxin production is sustained following N depletion by recycled NH_4^+ (McCarthy et al. 2007; Gardner et al. 2017; Hampel et al. 2018; this study). NH_4^+ regeneration rates were scaled by delineating the western basin into zones by station and calculating the volume of each station area (see Boedecker et al. 2020). NH_4^+ regenerated at each station was then compared to incoming TN loads from the Maumee River (NCWQR Heidelberg tributary monitoring program, https://ncwqr.org/monitoring/, last accessed 17 October 2020; Richards et al. 2010).

In 2015, NH_4^+ regeneration during the sampling season added NH_4^+ equivalent to 76% of the annual TN load and 160% of the TN load during the sampling period (June–September). Including August 2015, the internal NH_4^+ regeneration load increases to 2.2 times the annual TN load and 4.5 times the TN load during the sampling season. In 2016 and 2017, regenerated NH_4^+ contributed NH_4^+ equivalent to 60% of the annual TN load and 1.3–1.5 times the seasonal TN load (Table 3). When monthly NH_4^+ regeneration rates were summed to calendar year (using April 2016 rates as a proxy for winter months), NH_4^+ regeneration could supply 240–250% of the annual TN load in 2016 and 2017. This relative contribution ($\sim 2\times$) is similar to estimates for Missisquoi Bay (McCarthy et al. 2013), Lake Taihu (Hampel et al. 2018), and Sandusky Bay ($\sim 77\%$; Hampel et al. 2019*a*).

Sediments also contribute to water column N availability in aquatic ecosystems (An and Gardner 2002; McCarthy et al. 2016). Recent work at many of the same stations as the present study reported that western basin sediments release NH_4^+ and urea at rates equivalent to 4–11% of the annual TN load (Boedecker et al. 2020). Combined, water column and sediments (NH_4^+ release $\sim 11\%$ of water column NH_4^+ regeneration) represent a continuous supply of internal N when external N loads are minimal, cyanobacterial biomass is high, and water column N concentrations are depleted.

Despite high spring nutrient loading from the Maumee River, cyanoHABs do not develop in western Lake Erie until mid- or late-July, corresponding with higher water temperatures and proportion of chemically reduced N forms in the external N load (Newell et al. 2019). The ratio of microcystin to phycocyanin peaked when regenerated NH_4^+ was (up to 50 times) greater than the Maumee River TN load from the previous week ($F_{2,46} = 2.70$; $p = 0.020$; Supporting Information Fig. S9). This observation suggests a "sweet spot," where NH_4^+ regeneration supports biomass and toxin production, and biomass maintenance is favored over toxin production (Harke and Gobler 2013). When NH_4^+ regeneration exceeded weekly TN loading by >50 times (late August and September), toxin concentrations in biomass decreased and were not different from those when external loads were higher than internal loading (Supporting Information Fig. S9).

Although microcystins contain, on average, 10 N per molecule (Honkanen et al. 1990), there were no strong relationships between any N species and toxin concentrations in the present study. Given the high rates of NH_4^+ regeneration reported here, snapshot sampling to determine DIN concentrations do not accurately represent N availability. However, NH_4^+ regeneration and potential uptake rates are good proxies for N demand and bioavailability (Gardner et al. 2017). Thus, water column NH_4^+ cycling rates, previously missing from the literature for this and most other freshwater systems, may represent key parameters to consider when developing models to predict toxin concentrations in cyanoHAB impacted systems.

Conclusions

This study contributes to the growing body of literature highlighting the importance of NH_4^+ and chemically reduced N in eutrophic lakes affected by seasonal cyanoHABs, especially those comprised of non-N-fixing, toxin-producing taxa (e.g., *Microcystis*). Water column NH_4^+ regeneration rates met or exceeded external N loads in the western basin and help explain why non-N-fixing cyanoHABs proliferate despite minimal external N loading. These results reinforce the need to manage external N loading to mitigate growth and toxin production of non-N-fixing cyanobacteria (McCarthy et al. 2013, 2016; Gobler et al. 2016; Newell et al. 2019). External nutrient loads stimulate biomass and toxin production, which becomes the substrate for NH_4^+ regeneration when cells are grazed and/or remineralized in the water column (Gardner and Lee 1975; McCarthy et al. 2013) and sediments (McCarthy et al. 2016; Boedecker et al. 2020). Thus, while in-system turnover should be accounted for in management and modeling applications, reducing external nutrient loads from watersheds remains the key to mitigating the global proliferation of contemporary cyanoHABs that cannot fix atmospheric N and produce N-rich toxins.

Data Availability Statement

Data used for biogeochemical rate calculations are available from corresponding author DKH upon request. The authors confirm that other data supporting the findings of this study are available within the article and/or linked public databases and within supplementary materials.

References

An, S., and W. S. Gardner. 2002. Dissimilatory nitrate reduction to ammonium (DNRA) as a nitrogen link, versus denitrification as a sink in a shallow estuary (Laguna Madre/Baffin Bay, Texas). Mar. Ecol. Prog. Ser. **237**: 41–50.

Bates, D., Maechler, M., Bolker, B., Walker, S. and Haubo Bojesen Christensen, R., 2015. lme4: Linear mixed-effects models using Eigen and S4. R package version 1.1–7. 2014.

Blackburn, T. H. 1979. Method for measuring rates of NH_4^+ turnover in anoxic marine sediments, using a 15N-NH_4^+ dilution technique. Appl. Environ. Microbiol. **37**: 760–765.

Blomqvist, P., A. Pettersson, and P. Hyenstrand. 1994. Ammonium-nitrogen–A key regulatory factor causing dominance of non-nitrogen-fixing cyanobacteria in aquatic systems. Arch. Hydrobiol. **132**: 141–164.

Boedecker, A. R., D. N. Niewinski, S. E. Newell, J. D. Chaffin, and M. J. McCarthy. 2020. Evaluating sediments as an ecosystem service in western Lake Erie via quantification of nutrient cycling pathways and selected gene abundances. J. Great Lakes Res. **40**: 920–932.

Caperon, J., D. Schell, J. Hirota, and E. Laws. 1979. Ammonium excretion rates in Kaneohe Bay, Hawaii, measured by a 15 N isotope dilution technique. Mar. Biol. **54**: 33–40.

Chaffin, J. D., T. W. Davis, D. J. Smith, M. M. Baer, and G. J. Dick. 2018. Interactions between nitrogen form, loading rate, and light intensity on Microcystis and Planktothrix growth and microcystin production. Harmful Algae **73**: 84–97.

Chaffin, J. D., and others. 2021. The Lake Erie HABs Grab: A binational collaboration to characterize the western basin cyanobacterial harmful algal blooms at an unprecedented high-resolution spatial scale. Harmful Algae **108**: 102080.

Collos, Y., A. Vaquer, A. M. Johnston, V. Pons, B. Bibent, and S. Richard. 2001. Carbon fixation, ammonium uptake and regeneration in an equatorial lake: Biological versus physical control. J. Plankton Res. **23**: 263–270.

Cooperative Institute for Great Lakes Research; University of Michigan and NOAA Great Lakes Environmental Research Laboratory. 2019. Physical, chemical, and biological water quality monitoring data to support detection of Harmful Algal Blooms (HABs) in western Lake Erie, collected by the Great Lakes Environmental Research Laboratory and the Cooperative Institute for Great Lakes Research since 2012. [2015–2017]. NOAA National Centers for Environmental Information. Dataset. doi:10.25921/11da-3x54

Gardner, W. S., and G. F. Lee. 1975. The role of amino acids in the nitrogen cycle of Lake Mendota. Limnol. Oceanogr. **20**: 379–388.

Gardner, W. S., P. J. Lavrentyev, J. F. Cavaletto, M. J. McCarthy, B. J. Eadie, T. H. Johengen, and J. B. Cotner. 2004. Distribution and dynamics of nitrogen and microbial plankton in southern Lake Michigan during spring transition 1999–2000. J. Geophys. Res. Oceans **109**: 1–16.

Gardner, W. S., and others. 2017. Community biological ammonium demand: A conceptual model for cyanobacteria blooms in eutrophic lakes. Environ. Sci. Technol. **51**: 7785–7793.

Glibert, P. M., M. R. Dennett, and D. A. Caron. 1988. Nitrogen uptake and NH_4^+ regeneration by pelagic microplankton and marine snow from the North Atlantic. J. Mar. Res. **46**: 837–852.

Gilbert, P. M., F. P. Wilkerson, R. C. Dugdale, J. A. Raven, C. L. Dupont, P. R. Leavitt, A. E. Parker, J. M. Burkholder, and T. M. Kana. 2016. Pluses and minuses of ammonium and ntrate uptake and assimilation by phytoplankton and implications for productivity and community composition, with emphasis on nitrogen-enriched conditions. Limnol. Oceanogr. **61**: 165–197.

Gobler, C. J., J. M. Burkholder, T. W. Davis, M. J. Harke, T. Johengen, C. A. Stow, and D. B. Van de Waal. 2016. The dual role of nitrogen supply in controlling the growth and toxicity of cyanobacterial blooms. Harmful Algae **54**: 87–97.

Gu, B., and V. Alexander. 1993. Dissolved nitrogen uptake by a cyanobacterial bloom (Anabaena flos-aquae) in a subarctic lake. Appl. Environ. Microbiol. **59**: 422–430.

Hampel, J. J., M. J. McCarthy, W. S. Gardner, L. Zhang, H. Xu, G. Zhu, and S. E. Newell. 2018. Nitrification and ammonium dynamics in Taihu Lake, China: Seasonal competition for ammonium between nitrifiers and cyanobacteria. Biogeosciences **15**: 733–748.

Hampel, J. J., M. J. McCarthy, M. Neudeck, G. S. Bullerjahn, R. M. L. McKay, and S. E. Newell. 2019*a*. Ammonium recycling supports toxic Planktothrix blooms in Sandusky Bay, Lake Erie: Evidence from stable isotope and metatranscriptome data. Harmful Algae **81**: 42–52.

Hampel, J. J., M. J. McCarthy, M. H. Reed, and S. E. Newell. 2019*b*. Short term effects of Hurricane Irma and cyanobacterial blooms on ammonium cycling along a freshwater–estuarine continuum in south Florida. Front. Mar. Sci. **6**: 640.

Harke, M. J., and C. J. Gobler. 2013. Global transcriptional responses of the toxic cyanobacterium, Microcystis aeruginosa, to nitrogen stress, phosphorus stress, and growth on organic matter. PLoS One **8**: e69834.

Harke, M. J., T. W. Davis, S. B. Watson, and C. J. Gobler. 2016. Nutrient-controlled niche differentiation of western Lake Erie cyanobacterial populations revealed via metatranscriptomic surveys. Environ. Sci. Technol. **50**: 604–615.

Harrell, F. E., Jr. 2019. Package "Hmisc", v. **2019**. CRAN, p. 235–236.

Honkanen, R. E., J. Zwiller, R. E. Moore, S. L. Daily, B. S. Khatra, M. Dukelow, and A. L. Boynton. 1990. Characterization of microcystin-LR, a potent inhibitor of type 1 and type 2A protein phosphatases. J. Biol. Chem. **265**: 19401–19404.

Hopkinson, C. S., Jr., B. F. Sherr, and H. W. Ducklow. 1987. Microbial regeneration of ammonium in the water column of Davies Reef, Australia. Mar. Ecol. Prog. Ser. **41**: 147–153.

International Joint Commission (IJC), 1978. Great Lakes Water Quality Agreement. https://www.ijc.org/en/who/mission/glwqa

James, R. T., W. S. Gardner, M. J. McCarthy, and S. A. Carini. 2011. Nitrogen dynamics in Lake Okeechobee: Forms, functions, and changes. Hydrobiologia **669**: 199–212.

Jarvie, H. P., L. T. Johnson, A. N. Sharpley, D. R. Smith, D. B. Baker, T. W. Bruulsema, and R. Confesor. 2017. Increased soluble phosphorus loads to Lake Erie: Unintended consequences of conservation practices? J. Environ. Qual. **46**: 123–132.

Jiang, X., L. Zhang, G. Gao, X. Yao, Z. Zhao, and Q. Shen. 2019. High rates of ammonium recycling in northwestern Lake Taihu and adjacent rivers: An important pathway of nutrient supply in a water column. Environ. Pollut. **252**: 1325–1334.

Kana, T. M., C. Darkangelo, M. D. Hunt, J. B. Oldham, G. E. Bennett, and J. C. Cornwell. 1994. Membrane inlet mass spectrometer for rapid high-precision determination of N_2, O_2, and Ar in environmental water samples. Anal. Chem. **66**: 4166–4170.

Kumar, S., R. W. Sterner, and J. C. Finlay. 2008. Nitrogen and carbon uptake dynamics in Lake Superior. J. Geophys. Res. Biogeo. **113**: 1–15.

Kuniyoshi, T. M., A. Gonzalez, S. Lopez-Gomollon, A. Valladares, M. T. Bes, M. F. Fillat, and M. L. Peleato. 2011. 2-oxoglutarate enhances NtcA binding activity to promoter regions of the microcystin synthesis gene cluster. FEBS Lett. **585**: 3921–3926.

Lenth, R., Singmann, H., Love, J., Buerkner, P. and Herve, M., 2019. emmeans: Estimated marginal means, aka least-squares means (version 1.3.4).

Martin, J. F., and others. 2021. Evaluating management options to reduce Lake Erie algal blooms using an ensemble of watershed models. J. Environ. Manage. **280**: 111710.

McCarthy, M. J., P. J. Lavrentyev, L. Yang, L. Zhang, Y. Chen, B. Qin, and W. S. Gardner. 2007. Nitrogen dynamics and microbial food web structure during a summer cyanobacterial bloom in a subtropical, shallow, well-mixed, eutrophic lake (Lake Taihu, China). Hydrobiologia **581**: 195–207.

McCarthy, M. J., W. S. Gardner, M. F. Lehmann, and D. F. Bird. 2013. Implications of water column ammonium uptake and regeneration for the nitrogen budget in temperate, eutrophic Missisquoi Bay, Lake Champlain (Canada/USA). Hydrobiologia **718**: 173–188.

McCarthy, M. J., W. S. Gardner, M. F. Lehmann, A. Guindon, and D. F. Bird. 2016. Benthic nitrogen regeneration, fixation, and denitrification in a temperate, eutrophic lake: Effects on the nitrogen budget and cyanobacteria blooms. Limnol. Oceanogr. **61**: 1406–1423.

Morrissey, K. M., and T. R. Fisher. 1988. Regeneration and uptake of ammonium by plankton in an Amazon floodplain lake. J. Plankton Res. **10**: 31–48.

Murphy, T. P. 1980. Ammonia and nitrate uptake in the lower Great Lakes. Can. J. Fish. Aquat. Sci. **37**: 1365–1372.

Newell, S. E., T. W. Davis, T. H. Johengen, D. Gossiaux, A. Burtner, D. Palladino, and M. J. McCarthy. 2019. Reduced forms of nitrogen are a driver of non-nitrogen-fixing harmful cyanobacterial blooms and toxicity in Lake Erie. Harmful Algae **81**: 86–93.

Paerl, H. W., J. T. Scott, M. J. McCarthy, S. E. Newell, W. S. Gardner, K. E. Havens, D. K. Hoffman, S. W. Wilhelm, and W. A. Wurtsbaugh. 2016. It takes two to tango: When and where dual nutrient (N & P) reductions are needed to protect lakes and downstream ecosystems. Environ. Sci. Technol. **50**: 10805–10813.

Présing, M., S. Herodek, T. Preston, and L. Vörös. 2001. Nitrogen uptake and the importance of internal nitrogen loading in Lake Balaton. Freshw. Biol. **46**: 125–139.

Présing, M., P. Sprőber, A. W. Kovács, L. Vörös, G. Kenesi, T. Preston, A. Takátsy, and I. Kóbor. 2008. Phytoplankton nitrogen demand and the significance of internal and external nitrogen sources in a large shallow lake (Lake Balaton, Hungary). Hydrobiologia **599**: 87–95.

R Core Team, 2020. R: A language and environment for statistical computing. R Foundation for Statistical Computing,. Available from https://www.R-project.org/.

Richards, R. P., D. B. Baker, J. P. Crumrine, and A. M. Stearns. 2010. Unusually large loads in 2007 from the Maumee and Sandusky Rivers, tributaries to Lake Erie. J. Soil Water Conserv. **65**: 450–462.

River, M., and C. J. Richardson. 2019. Dissolved reactive phosphorus loads to western Lake Erie: The hidden influence of nanoparticles. J. Environ. Qual. **48**: 645–653.

Steffen, M. M., B. S. Belisle, S. B. Watson, G. L. Boyer, and S. W. Wilhelm. 2014. Status, causes and controls of cyanobacterial blooms in Lake Erie. J. Great Lakes Res. **40**: 215–225.

Takamura, N., T. Iwakuma, and M. Yasuno. 1987. Uptake of ^{13}C and ^{15}N (ammonium, nitrate and urea) by Microcystis in Lake Kasumigaura. J. Plankton Res. **9**: 151–165.

Van de Waal, D. B., V. H. Smith, S. A. Declerck, E. C. Stam, and J. J. Elser. 2014. Stoichiometric regulation of phytoplankton toxins. Ecol. Lett. **17**: 736–742.

Wallace, B. B., M. C. Bailey, and D. P. Hamilton. 2000. Simulation of vertical position of buoyancy regulating Microcystis aeruginosa in a shallow eutrophic lake. Aquat. Sci. **62**: 320–333.

Watson, S. B., and others. 2016. The re-eutrophication of Lake Erie: Harmful algal blooms and hypoxia. Harmful Algae **56**: 44–66.

Wynne, T. T., R. P. Stumpf, R. W. Litaker, and R. R. Hood. 2021. Cyanobacterial bloom phenology in Saginaw Bay from MODIS and a comparative look with western Lake Erie. Harmful Algae **103**: 101999.

Yin, G., L. Hou, M. Liu, Z. Liu, and W. S. Gardner. 2014. A novel membrane inlet mass spectrometer method to

measure $^{15}NH_4^+$ for isotope-enrichment experiments in aquatic ecosystems. Environ. Sci. Technol. **48**: 9555–9562.

Acknowledgments

This research was funded by Ohio Sea Grant. We thank the NOAA Great Lakes Environmental Research Laboratory and the Cooperative Institute for Great Lakes Research, along with their boat captains, for providing sampling opportunities aboard their vessel. The authors appreciate comments and suggestions from colleagues at Bowling Green State University and the helpful perspective on statistical approaches provided by Megan Rúa and Molly Simonis. Additional thanks to Justin Chaffin at The Ohio State Stone Laboratory for sampling assistance in 2016, and to Chad Hammerschmidt for his comments on early drafts. The authors are grateful to Justyna Hampel, Erica Strope, Megan Reed, and all other Newell/McCarthy lab students and colleagues for assistance with sample collection and processing. The authors dedicate this work to Dr. Wayne S. Gardner in recognition of his decades-long advocacy for the importance of understanding nitrogen cycling in lakes and, specifically, the Laurentian Great Lakes.

Submitted 30 September 2021
Revised 08 April 2022
Accepted 20 June 2022

Associate editor: K. David Hambright, Yong Liu